

# Local strain-driven migration of oxygen vacancies to apical sites in $\text{YBa}_2\text{Cu}_3\text{O}_{7-x}$

Bernat Mundet<sup>a,†,‡</sup>, Steven T. Hartman<sup>b,‡</sup>, Roger Guzman<sup>a</sup>, Juan C. Idrobo<sup>c</sup>, Xavier Obradors<sup>a</sup>, Teresa Puig<sup>a</sup>, Rohan Mishra<sup>d,\*</sup>, Jaume Gázquez<sup>a,\*</sup>

<sup>a</sup>Institut de Ciència de Materials de Barcelona (ICMAB-CSIC), Campus UAB, Bellaterra, 08193 Barcelona, Spain

<sup>b</sup>Institute of Materials Science and Engineering, Washington University in St. Louis, St. Louis, Missouri 63130, United States

<sup>c</sup>Center for Nanophase Materials Sciences, Oak Ridge National Laboratory, Oak Ridge, Tennessee 37831, USA

<sup>d</sup>Department of Mechanical Engineering and Materials Science, Washington University in St. Louis, St. Louis, Missouri 63130, United States

This .pdf file contains additional information supporting the main text regarding the following points.

## Microstructural details

### *YBCO films' microstructure*

**Figure S1a and S1b** are low magnification HAADF images of a pristine YBCO thin film and a nanocomposite YBCO thin film, containing randomly oriented and homogeneously distributed BaZrO<sub>3</sub> nanoparticles, both of them grown following the MOD route. Although a different microstructure is identified in each film, they always feature dark stripes running horizontally, which corresponds to the Y124 intergrowth defect. In the pristine case, the Y124 intergrowths are mainly confined at either the film's or substrate's surface, whereas the homogeneously dispersed BZO NP's that are trapped within the nanocomposite film trigger the generation of Y124 intergrowths everywhere.

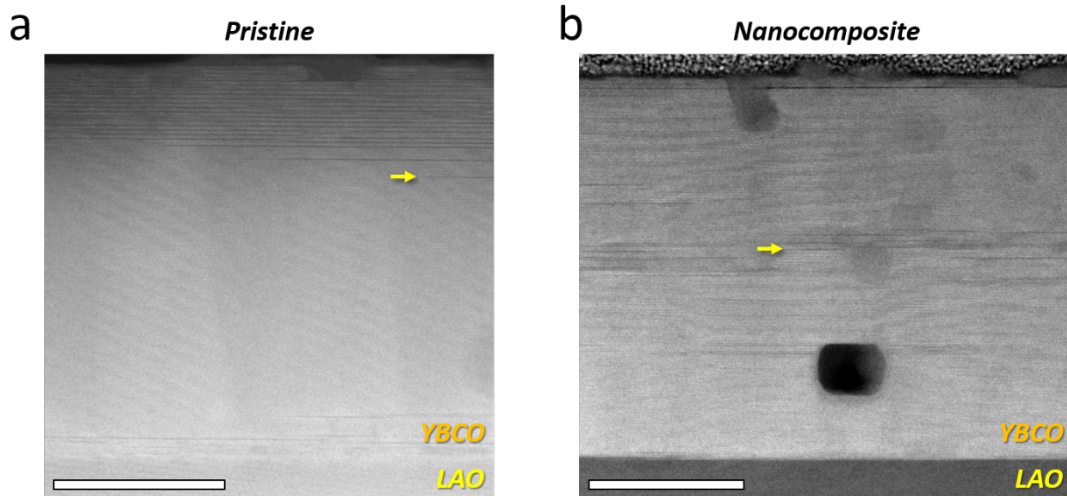


**Figure S1.** Low magnification HAADF image of a (a) pristine and (b) nanocomposite YBCO thin film. The yellow arrows point to Y124 intergrowths. Scale bars: 100nm.

### *Y124 intergrowth structure*

**Fig. S2a and S2b** are HAADF images showing a Y124 intergrowth that is viewed along either the *a*- or *b*-axes, respectively. The corresponding view of the Y124 structure is also superimposed onto each HAADF image. Notice that the Y123 structure is shifted half unit cell along the basal direction only when the structure is viewed along the  $\langle 100 \rangle$  zone axis (**Fig. S2b**), leading to a non-conservative stacking fault with a displacement vector of  $\frac{1}{2} [0\ 1\ c/3]$ . **Fig. S2c** displays the edge of a Y124 intergrowth defect, being the dashed yellow line the approximate position where the Y123 and Y124 structures are connected through a partial dislocation. Therefore, the Y124 intergrowth can be considered as a Frank loop dislocation, this is an extrinsic stacking fault surrounded by a partial dislocation. Strong strain fields are localized around this partial dislocation, where an additional Cu-O chain layer have to be inserted between the two neighboring BaO planes.

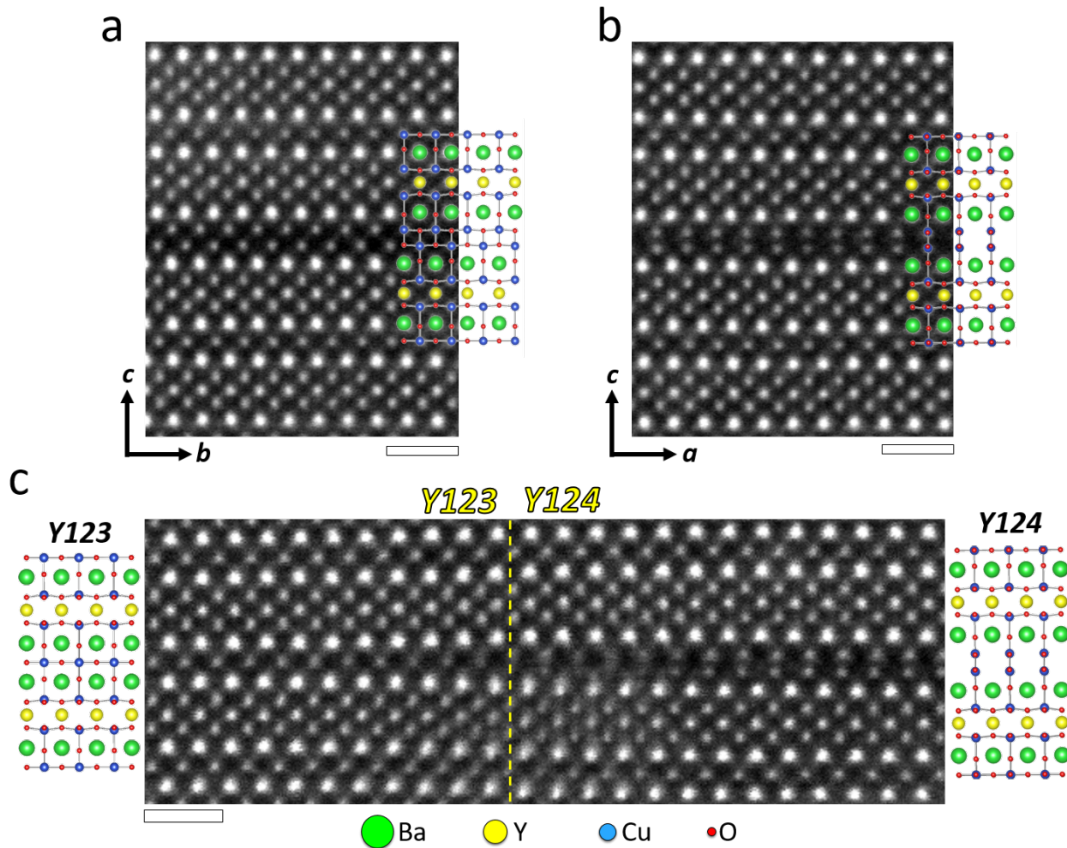


**Figure S2.** High resolution HAADF image of a Y124 intergrowth when viewed along the (a)  $\langle 100 \rangle$  and (b)  $\langle 010 \rangle$  zone axes. The superimposed structures correspond to the Y124 one viewed along the corresponding zone axis. (c) HAADF image showing the edge of a Y124 intergrowth. The dashed yellow line represents the position where both the Y123 and Y124 structures are connected through a partial dislocation. Scale bars: 1 nm.

### *YBCO single crystal microstructure*

**Figure S3a** shows a low magnification HAADF image of the surface of a YBCO single crystal sample. The brighter region corresponds to the YBCO sample whereas the upper darkest areas are the protecting Pt layers that are needed for the lamella specimen preparation process. Notice that the image contrast of the crystal area located deep below the surface is homogeneous signaling the absence of crystalline defects, whereas some image blurring is identified at the single crystal surface. A larger magnification image of this particular region (red square) is displayed in **Figure S3b**. It can be seen that this blurring effect is caused by the presence of numerous dark stripes running horizontally, which corresponds to the Y124 intergrowth defect. In particular, it is observed that these defects are only confined at the first 100-200 nm of the crystal below the surface.

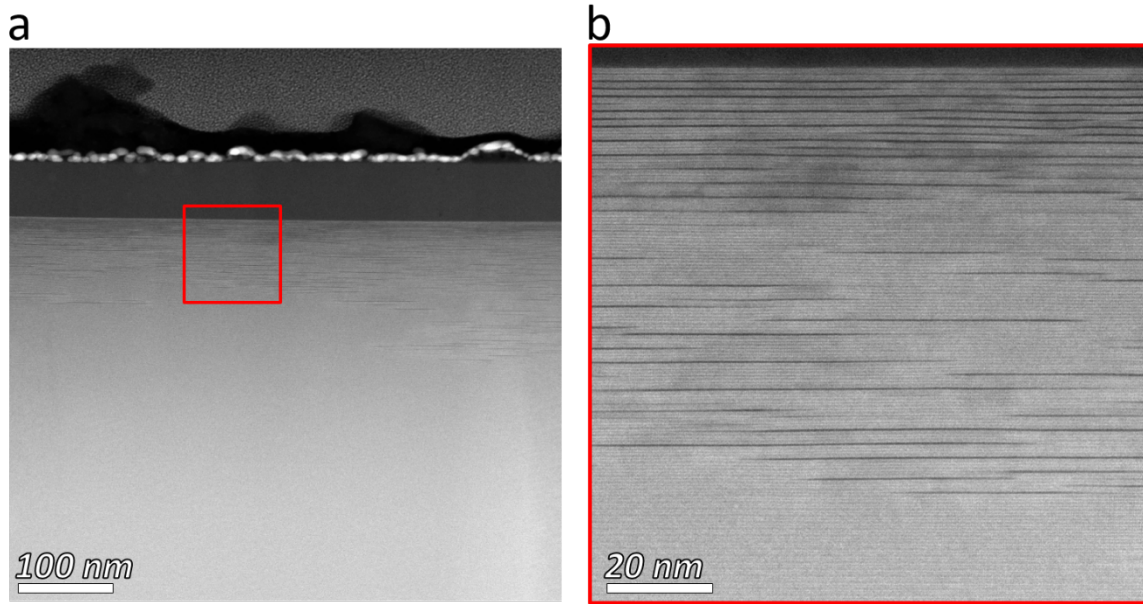


**Figure S3.** Low magnification HAADF image of the surface of a YBCO single crystal sample. The red square region of Fig. S2a is displayed with a larger resolution in Fig. S2b showing the presence of numerous Y124 intergrowths (dark stripes) within the first 100-200 nm of the single crystal.

### *c*-axis mapping

In the main manuscript, we have evaluated how the YBCO *c*-axis parameter, i.e. the *c*-axis strain, changes along the *c*-axis direction in those YBCO unit cells located at either side of one (or two) Y124 intergrowth defect. This study has been performed by calculating the *c*-axis spacing between the neighboring and heaviest atomic columns (Ba and Y) that are imaged in the HAADF image that is shown in **Fig. S4a** (or **Fig. 4** in the main manuscript). Prior to these calculations, we have first identified the central position of each Y and Ba atomic columns by using an iterative process, possessing picometer resolution, that localizes the center of mass position of each atomic spot. Once this identification process is concluded, we subtract the out-of-plane coordinate of two neighboring atomic columns, both located at the same in-plane position, repeating this step for all the imaged columns. This process allows us to obtain the *c*-axis map that is shown in **Fig. S4b**, where each square corresponds to either a Y-Ba, Ba-Ba or Ba-Y spacing and each square color correlates with its corresponding *c*-axis spacing. Notice that the Ba-Ba spacing is clearly distinguished from the Ba-Y and Y-Ba ones, as it appears in green in contrast to the other spacings whose color is blue. Besides, each Y124 intergrowth is easily identified as a yellow line in this map as a result of the out-of-plane lattice expansion occurring there. On the other hand, a subtle lattice compression (blue color) can be also noticed in those lines adjoining the faults, whose blue contrast become more intense than the non-distorted Ba-Y spacings. By averaging several unit cells from the same atomic row, we have calculated the *c*-axis profiles that are shown in Fig.4a

of the main manuscript, where all the lattice distortions occurring near the faults can be clearly observed.

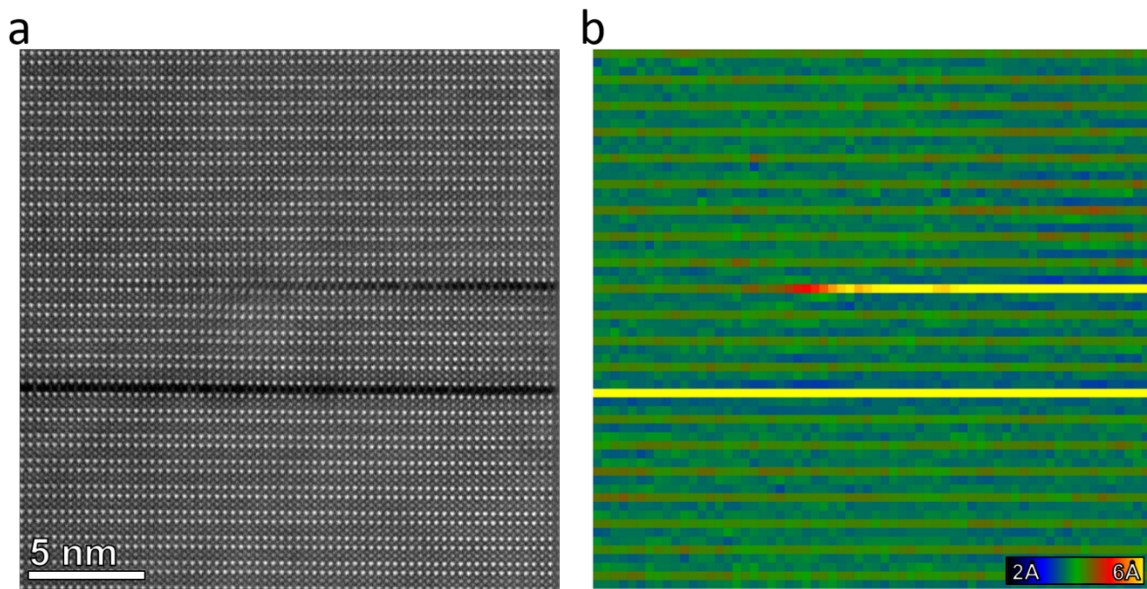


**Figure S4.** (a) High-magnification HAADF image of the YBCO crystal containing two Y124 intergrowths. Its corresponding Y-Ba, Ba-Ba and Ba-Y c-axis map is shown in (b), where each pixel represents the image position of one of these spacings and its color scales with its corresponding c-axis spacing.